

MATERIALS LABORATORY REPORT

Course Title: **ME1 Engineering Materials**

Report Title: **Properties of Engineering Alloys**

Author: **Rishi Kumra**

Group: **5d**

Date of Experiment: **2/02/2017**

Department of Mechanical Engineering
Imperial College London
2016 – 2017

Abstract

Aluminium and steel are major components of a large range of commercial products used every day. Therefore, it's ever more important to study the effects of different compositions and chemical processing on the mechanical properties of these materials. This report details two investigations:

- 1) Study of the tensile behaviour of various aluminium and aluminium alloy samples as a function of their composition and processing history
- 2) Investigation into the effect of hypo-eutectoid steel's carbon content on the hardness of steels

In the first investigation, five aluminium specimens were placed in a standard tensile testing machine and tested to failure. Each specimen was processed differently. There was a pure aluminium sample, a cold-worked pure aluminium sample, a magnesium-aluminium alloy and two samples that had been heat treated (precipitation hardened at different temperatures – optimum temperature and a very high temperature). Results showed that temperature had a significant impact on strength – the material precipitation hardened at a very high temperature was much weaker than the optimally treated material. The highest UTS (Ultimate Tensile Strength) was recorded by the sample that was precipitation hardened at the optimum temperature. In addition, it was the stiffest material, but also the most brittle. The experiment showed that work hardening, heat treatment and alloying increased the strength of aluminium at the cost of ductility.

In the second investigation, three hypo-eutectoid steel samples of 0.1%, 0.4% and 0.75% carbon weight were polished, etched and then the grain structure of each sample was examined underneath a microscope. All the samples were tested for hardness on a Vickers Hardness machine. The test indicated a positive correlation between carbon content and hardness (and therefore strength). This trend was further verified by microscopic analysis. Estimates of the amount of pearlite and ferrite in samples were calculated using the Lever rule. In terms of application, recommendations made include using 0.3% carbon steel for the welded footbridge (compromise between hardness and ductility), using 0.6% carbon steel with heat treatments for the crankshaft (to increase strength) and using 0.7% carbon steel with heat treatments (to increase strength) and cold working (to increase toughness) for the two parts of the chisel (the tip and the bottom).

Table of Contents

| | |
|------------------------------------|-----------|
| Abstract..... | i |
| Introduction | 1 |
| Materials and Methods | 2 |
| Results..... | 8 |
| Discussion | 12 |
| Conclusion | 17 |
| Appendices..... | 18 |
| References | 19 |

Introduction

The purpose of the investigation was to investigate the behaviour and structure of different types of aluminium and steel. Accordingly separate experiments were conducted for each of the two materials.

The first experiment investigated the tensile behaviour of various aluminium and aluminium alloy samples as a function of their composition and processing history. Aluminium is a major component of a range of commercial light alloys. This experiment illustrated the ways in which aluminium could be strengthened by mechanical working, alloying and heat treatment. A tensile test is convenient for determining the ductility, strength and toughness of a material, hence this test provided a general overview of the mechanical properties of each specimen. Five specimens were tested in tension and the strength and percentage elongation of each was then measured. In addition, the fracture angle and fracture sound of each specimen was observed and the 1% proof stress calculated. To find some of these values, force-displacement and stress-strain graphs were plotted.

The second investigation illustrated that steel's mechanical properties are dependent on the chemical composition and on the mechanical/ thermal treatments applied. Despite several alloying elements being present in steel, carbon is the most significant in its impact on the structure and properties of steel. The aim of this experiment was to investigate the hardness and microstructure of three samples of slowly cooled carbon steel. The aim was to also provide a recommendation on which types of steel to use for various applications: a welded footbridge, a chisel and a crankshaft. The hardness of steels with different carbon contents was determined by carrying out a Vickers hardness test. This test was carried out using a benchtop Vickers hardness machine and a computer for steel samples with different carbon contents. In addition to hardness being affected by carbon content, the microstructure of steel changes as it undergoes phase changes during mechanical/ thermal treatment processes. To study the microstructure of the annealed steel samples, they were first polished, washed dried and etched. This coloured the steel samples – displaying an observable contrast in the different phases present in steel alloys of 0.1, 0.4 and 0.75 % wt% carbon (hypo-eutectoid steels). Relative proportions of the phases present were estimated and then compared to the proportions obtained using the Lever rule (equation 1). This led to a determination of the relationship between carbon content and the effect on the microstructures of different steel alloys.

$$M_{\alpha_p} = \frac{C_{Pearlite} - X}{C_{Pearlite} - C_{\alpha_p}} \quad (1)$$

where M_{α_p} is the fraction of ferrite in a steel sample with carbon content X

Materials and Methods

The first experiment involved a conventional tensile test of various aluminium specimens; measurements of UTS, % elongation, proof stress (1%), fracture sound and fracture angle were obtained from the test. The second experiment involved a Vickers Hardness test of three samples of steel, followed by the study of microstructures (using an optical microscope) of each of the samples of steel after being polished and etched.

Safety precautions:

Necessary precautions include wearing lab coats and safety goggles, removing trip hazards and tying long hair back to protect the eyes from damage that may occur due to the failure of the machines and to help avoid accidents with the machines.

Experiment 1 – Tensile behaviour of aluminium and its alloys

Apparatus:

- 1) Instron bench top test machines (crosshead speed of $5 \frac{\text{mm}}{\text{min}}$ and $\pm 0.5\%$ uncertainty in Load and Extension)

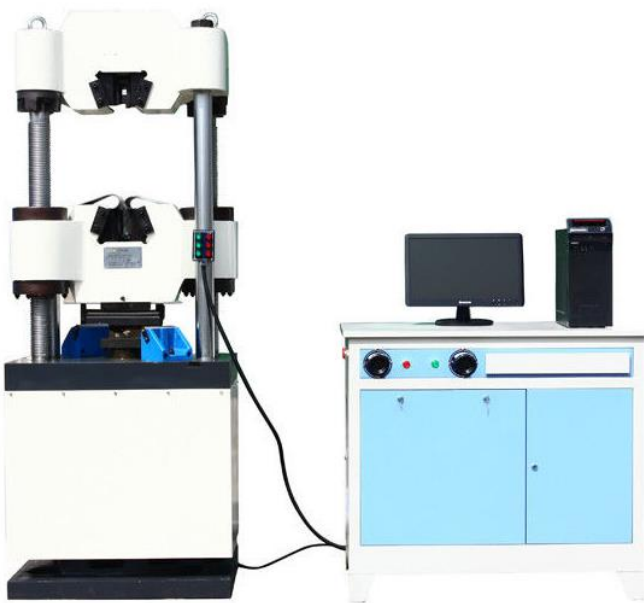


Figure 1 & 2. Universal Tensile Testing Machine (source: in References section)

- 2) Micrometer ($\pm 0.005\text{mm}$)

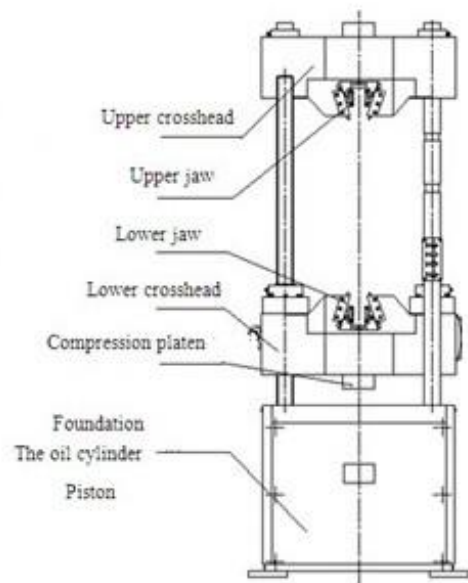


Figure 3. Labelled Universal Tensile Testing Machine

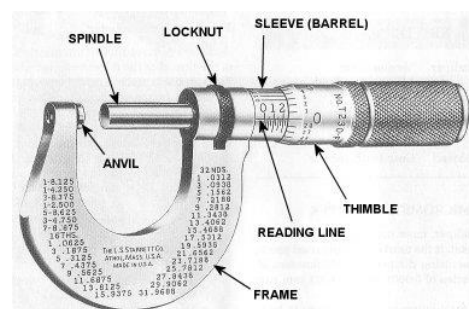


Figure 4. Micrometer Screw Gauge

3) Vernier Calliper ($\pm 0.005\text{mm}$)

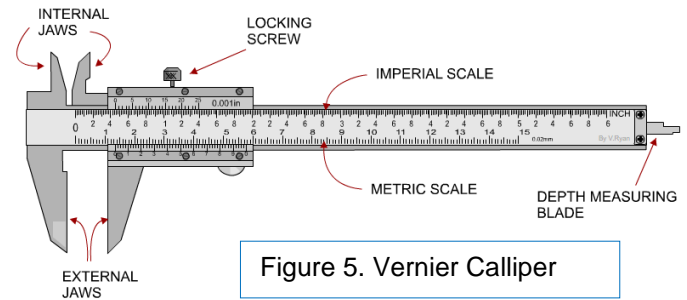


Figure 5. Vernier Calliper

4) Aluminium tensile test specimen (x5)



Figure 6. Test specimen

Method:

The experiment was conducted in the following steps.

- 1) The five aluminium specimens were marked with various colours: blue, pink, red, green and black as follows:

Table 1: Coded aluminium samples with different alloy compositions and treatments (Blackman, 2016)

| # | Code | Description, composition, treatment. |
|---|--------|--|
| 1 | Black | Pure Aluminium – fine grained, annealed. Grade 1200-O; 99% Al, (Max 0.1% Cu, 0.5% Si, 0.7% Fe, 0.1% Mn, 0.1% Zn). |
| 2 | Yellow | Pure Aluminium – fine grained, cold worked. Grade 1200-H14; <i>Composition as above but fully work hardened by cold rolling.</i> |
| 3 | Red | Aluminium / Magnesium – annealed. Grade 5251-O; 1.8-2.4% Mg, 0.5% Mn, otherwise similar to above, remainder Al. <i>This alloy is a single phase substitutional solid solution.</i> |
| 4 | Green | Aluminium – 4% Cu alloy. (Often called 'Duralumin') Grade 2014A-T6; 4.4% Cu, 0.5% Mg, 0.8% Si, 0.8% Mn, remainder Al. <i>This alloy has a two phase structure and has been heat treated by a two stage process (solution treatment and precipitation hardening) to produce maximum strengthening. The precipitation hardening took place at 250 °C for 1 hour.</i> |
| 5 | Orange | Aluminium – 4% Cu alloy. Grade- Nominally the same as #4 <i>This alloy has a two phase structure but has been deliberately given an incorrect heat treatment. It has been solution treated as for #4 but then overaged at 400 °C for 1 hour instead of the correct precipitation treatment.</i> |

- 2) The gauge length of each sample was measured using a Vernier Calliper (figure 5). After three measurements were made, an average gauge length was calculated (ignoring anomalies). The width of each of the samples were also measured three times using a Vernier Calliper and an average width was calculated. Uncertainty in each of the measurements of width and gauge length = $\pm 0.005\text{mm}$. The thickness of each sample was then measured three times using a micrometer (figure 4) and an average thickness was calculated. Using the values for width and thickness of each

sample, the cross-sectional area of each specimen and the uncertainty was calculated.

$$Area = Thickness * Width \quad (2)$$

- 3) The aluminium alloy specimen (figure 6), known gauge length, was placed into the testing machine (figure 1/2/3) using a screw-driven system and a real-time load-extension graph was displayed. Sample was tested to failure. The necking of the specimen, fracture sound and angle of fracture was observed as the specimen extended. The load-extension graph was analysed and readings for the maximum load (top point of graph) were taken. Load was given with an uncertainty of $\pm 1\%$.
- 4) By using the values for maximum load in *step 2* and value for cross-sectional area in *step 2*, the UTS and its uncertainty was calculated, where:
(Appendix A – 1)

$$Stress (Pa) = \frac{force}{area} \quad \text{or} \quad \sigma = \frac{F}{A} \quad (3)$$

- 5) Next, proof stress was estimated using graph analysis. The force-extension graph was converted into a stress-strain graph using the equations for engineering stress (eqn #3) and engineering strain:

$$Strain = \frac{extension}{original length} \quad \text{or} \quad \epsilon = \frac{\Delta l}{l} \quad (4)$$

- 6) A trendline was added to the elastic region of the stress-strain curve and a linear equation for the elastic region of the curve was displayed. The proof stress at 1% is a strain offset of 0.01. Therefore, the linear equation was changed to include the offset of 0.01 (ie $y = k(x-0.01) + c$) and this new linear equation was plotted against the original curve. The point at which the new line intersects the original curve is the proof stress. For example, the green specimen has a proof stress of approximately 412 MPa:

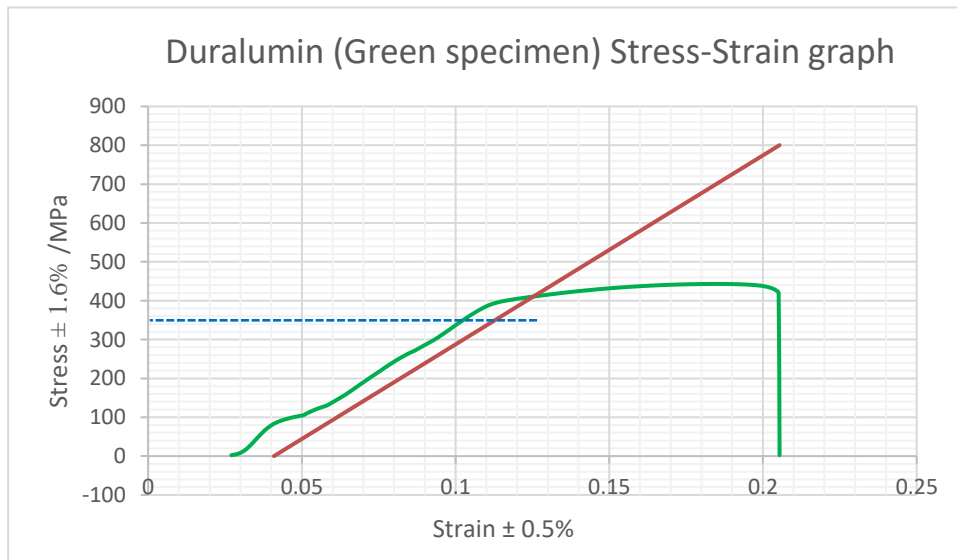


Figure 7 – Proof stress estimation 412 ± 6 MPa

- 7) Step 5 was repeated for all five specimens.
- 8) Once the specimen fractured, it was carefully taken out of the tensile testing machine. The final gauge length was measured using a Vernier calliper ($\pm 0.005\text{mm}$). This measurement was repeated three times and an average gauge length calculated. The final and initial gauge lengths of each specimen were used to calculate percentage elongation of the specimen:

$$\text{Percentage Elongation} = \frac{\text{Final Gauge Length} - \text{Initial Gauge Length}}{\text{Initial Gauge Length}} * 100 \quad (5)$$

Whilst Vernier callipers are precise to 0.01 mm, it's important to note that there was an additional uncertainty. After fracture, the aluminium specimen splits into two parts. Manually placing the two parts next to each other introduces a random error in the measurement of the final gauge length – the arrangement would vary slightly from person to person. Additionally, estimating proof stress from the stress-strain graph introduces an error in its value (approximately $\pm 5 \text{ MPa}$).

Experiment 2 – Investigating the hardness and microstructure of 'slowly cooled' carbon steel

Apparatus:

- 1) Bakelite Mounts (hold the specimens firmly whilst being polished)



Figure 8 -Bakelite Mounts

- 2) Hypo-eutectoid steel specimens

- 3) 2% Nital solution (concentrated nitric acid in methyl alcohol)



Figure 9 – 2% Nital solution

- 4) Polisher machine (two discs)



Figure 10 -Dual specimen polisher

- 5) Vickers Hardness machine and computer (unit of hardness = Vickers Pyramid Number HV)

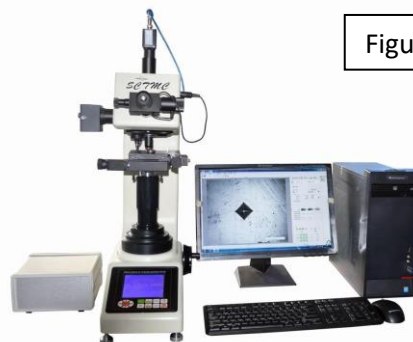


Figure 11 – Vickers Hardness Machine

Method:

- 1) The three steel samples were prepared by polishing, washing and etching.
 - i) The samples were mounted in Bakelite mounts (figure 8), which held the samples firmly in place. The samples were held in the centre of the polisher discs and pushed down. One disc polished particles which were $3\ \mu\text{m}$ and bigger, the other disc polished particles up to $1\ \mu\text{m}$ in size.
 - ii) Each sample was first placed in the centre of the $3\ \mu\text{m}$ disc, held down for 10 seconds and then lifted, washed and dried. Then, each sample was rotated 90° and placed face down on the $1\ \mu\text{m}$ disc.
 - iii) Next, the samples were etched by spreading 2% Nital solution across the face of each specimen. This clearly displays the different phases existent within the microstructure of the steel samples.
- 2) The specimens were examined microscopically and the regions of ferrite (light) and pearlite (dark and lamellar) were identified. The fraction of ferrite and pearlite in each sample was estimated. The theoretical fraction was then determined using the lever rule and steel's equilibrium phase diagram.

$$X_{\alpha p} = \frac{C_{\text{pearlite}} - \% \text{carbon content in sample}}{C_{\text{pearlite}} - C_{\alpha}} \quad (6)$$

and

$$X_{\text{pearlite}} = \frac{\% \text{carbon content in sample} - C_{\alpha}}{C_{\text{pearlite}} - C_{\alpha}} \quad (7)$$

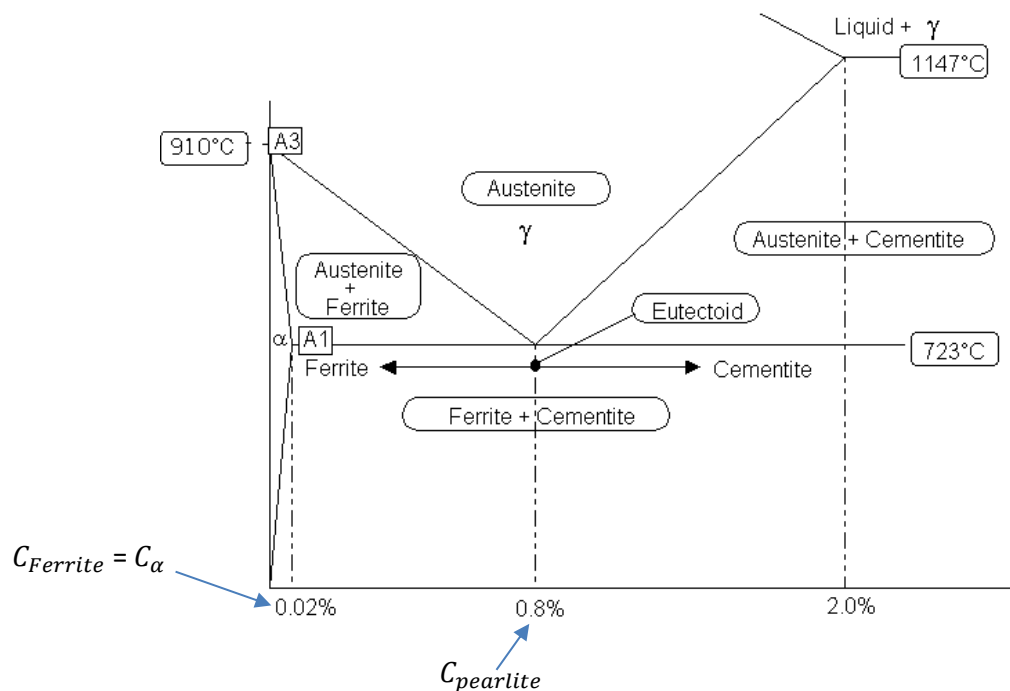


Figure 12 – Steel equilibrium phase diagram

- 3) The Vickers Hardness number (VH10) of each specimen was found using a benchtop Vickers hardness machine. The specimen was placed on the top plate and the lens focused till the face of the specimen was clearly displayed on the computer. The specimen was moved underneath the indenter, and the test started.
- 4) The diamond indenter produces a small hole in the specimen. The machine measures the diagonal length of the hole formed and produces a value for the Vickers hardness number of the specimen. This was repeated three times for each sample and the mean value was found.
- 5) The error associated with the Vickers Hardness machine is negligible relative to the random errors during the repeat measurements. Therefore, the absolute error for each value is found by:

$$\text{Absolute error in mean value} = \frac{\text{maximum value} - \text{minimum value}}{n} \quad (8)$$

Where $n = 3$ since three measurements were made for each specimen.

- 6) A graph of Vickers Hardness number vs Carbon Content was drawn, accounting for the error bars and maximum and minimum gradient lines.

Results

Experiment 1 - Tensile behaviour of aluminium and its alloys

- 1) The gauge length of each specimen was measured to be 22mm (± 0.005 mm). The average thickness and width were measured as below. The uncertainty analysis for cross-sectional area can be found in Appendix A-1.

2)

Table 2 – Results for thickness, width and cross-sectional area

| Colour | Average thickness (± 0.005 mm) | Average width (± 0.005 mm) | Cross-sectional area (mm^2) |
|--------|-------------------------------------|---------------------------------|--|
| Blue | 1.37 | 7.44 | 10.19 ± 0.04 |
| Pink | 1.13 | 7.66 | 8.66 ± 0.04 |
| Red | 0.91 | 7.47 | 6.80 ± 0.04 |
| Green | 0.94 | 7.47 | 7.02 ± 0.04 |
| Black | 1.02 | 7.45 | 7.60 ± 0.04 |

- 3) The load extension graphs for each specimen were produced in real-time during the tensile test. These graphs were compiled onto one Excel graph to compare the properties of the five aluminium samples (figure 13)

Specimen 1 to 5

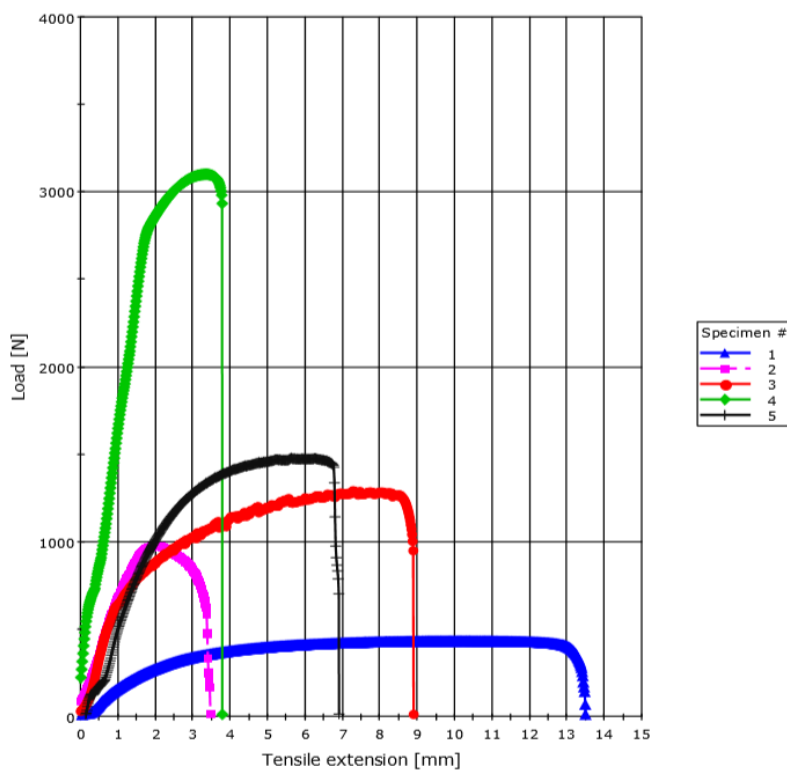


Figure 13 – Load-Extension graph for the five specimens, where specimen 1 is the blue sample, specimen 2 is the pink sample, specimen 3 is the red sample, specimen 4 is the green sample and specimen 5 is the black sample.

- 4) The maximum load value was found as the maximum point on the load-extension graph. The UTS is the maximum value of stress on the stress-strain curve. So all the graphs were first converted into stress-strain curves using engineering stress-strain values:

For the green sample, given load-extension values:

$$\text{Stress (MPa)} = \frac{\text{Load}}{\text{Area}} = \frac{\text{Load}}{7.02} \quad \text{and} \quad \text{Strain} = \frac{\text{extension}}{\text{original length}} = \frac{\text{extension(mm)}}{22} \quad (3 \text{ \& } 4)$$

For the green sample, the stress-strain curve:

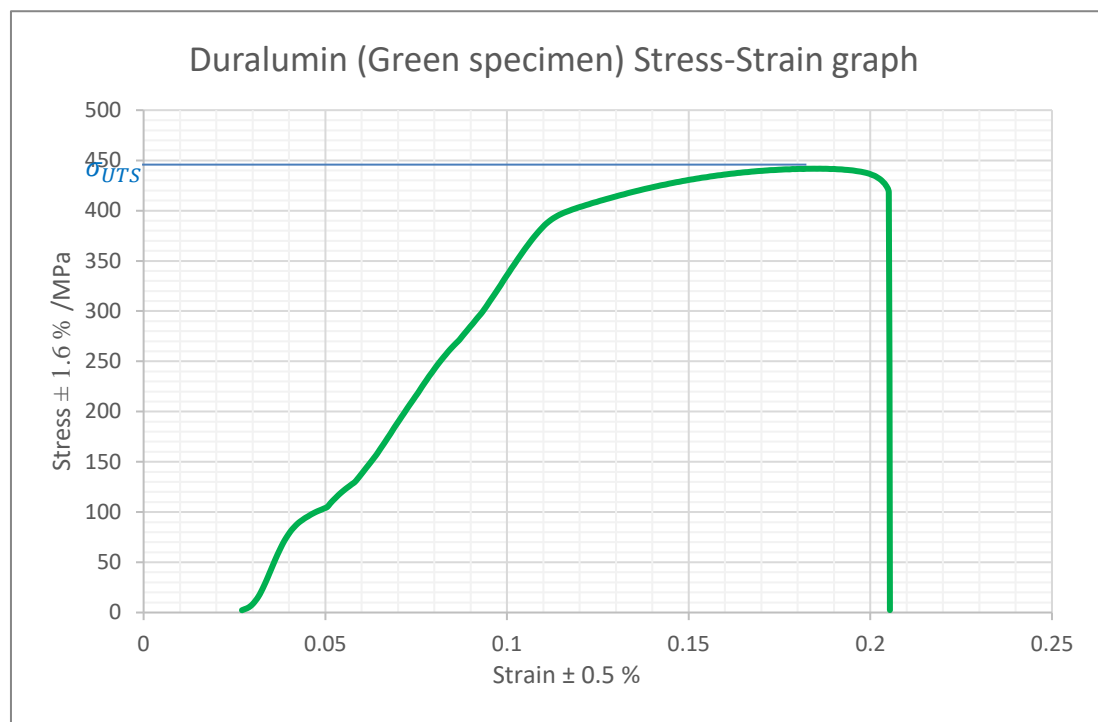


Figure 14 – Stress-Strain curve with the UTS estimated as 445 ± 7.1 MPa

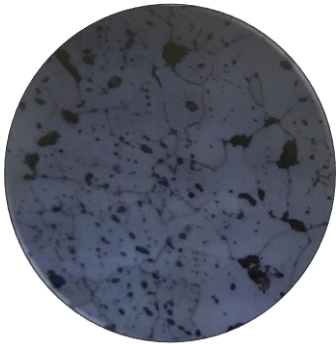
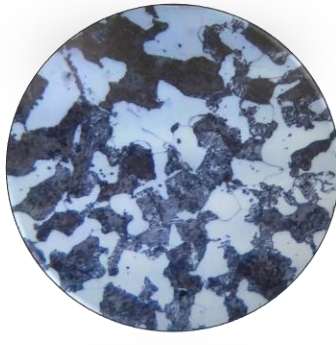
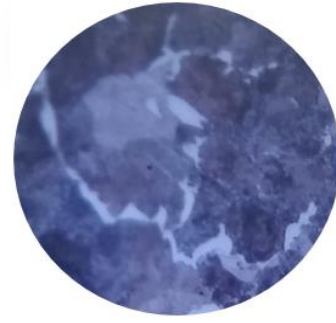
The UTS values for each of the specimens is found in Appendix B.

- 5) Next, the 1% proof strength for each of the specimens was estimated from the stress-strain graphs. Using Excel, the line equation $f(x)$ of the elastic region of the stress-strain curve was found. Then, a parallel line was drawn by using the transformation $f(x-0.01)$. The proof stress estimations can be found in Appendix B.
- 6) The necking and fracture shape of each specimen was observed carefully, described by the angle of fracture which varies from 45 to 90 degrees. In addition, the sound at fracture was noted. These results can be found in Appendix B.
- 7) Percentage elongation is a measure of ductility (a mechanical property). The percentage elongation was calculated for each specimen using the values for initial gauge length and final gauge length (eqn #5). These results can be found in Appendix B.

Experiment 2 - Investigating the hardness and microstructure of 'slowly cooled' carbon steel

1) After being prepared by polishing, washing and etching, the steel samples were examined under an optical microscope. The phase differences were clearly visible because of the Nital solution. From the view of the microstructure, reasonable estimates were made of the fraction of ferrite and pearlite (table below). Then, theoretical values were derived using the Lever rule (Appendix A-3)

Table 3 – Estimating regions of ferrite and pearlite in each of the three specimens

| Carbon Content | Sketch/Picture | Pearlite Estimate | Ferrite Estimate | Theoretical Pearlite % (Lever rule) | Theoretical Ferrite % (Lever rule) |
|----------------|---|-------------------|------------------|-------------------------------------|------------------------------------|
| 0.1 % |  | 10 | 90 | 10.26 | 89.74 |
| 0.4 % |  | 50 | 50 | 48.72 | 51.28 |
| 0.75 % |  | 95 | 5 | 93.59 | 6.41 |

2) The Vickers Hardness test was carried out on the three samples. The machine provided a VH 10 value to each specimen as shown below:

Table 4 – Results of the Vickers Hardness Test

| wt% C | Vickers Hardness (HV10) | | | | Uncertainty | %Uncertainty |
|-------|-------------------------|-------|-------|---------|-------------|--------------|
| | 1 | 2 | 3 | Average | | |
| 0.1 | 173.3 | 180.1 | 178.7 | 177.37 | 2.27 | 1.3 |
| 0.4 | 232.4 | 227.8 | 239.9 | 233.37 | 4.03 | 1.7 |
| 0.75 | 259.9 | 276.2 | 278.1 | 271.4 | 5.43 | 2.0 |

3) Using the data in table 4, accounting for the error bars associated with the repeat measurements, a graph of carbon content was plotted against Vickers Hardness. As expected, the graph was linearly proportional:

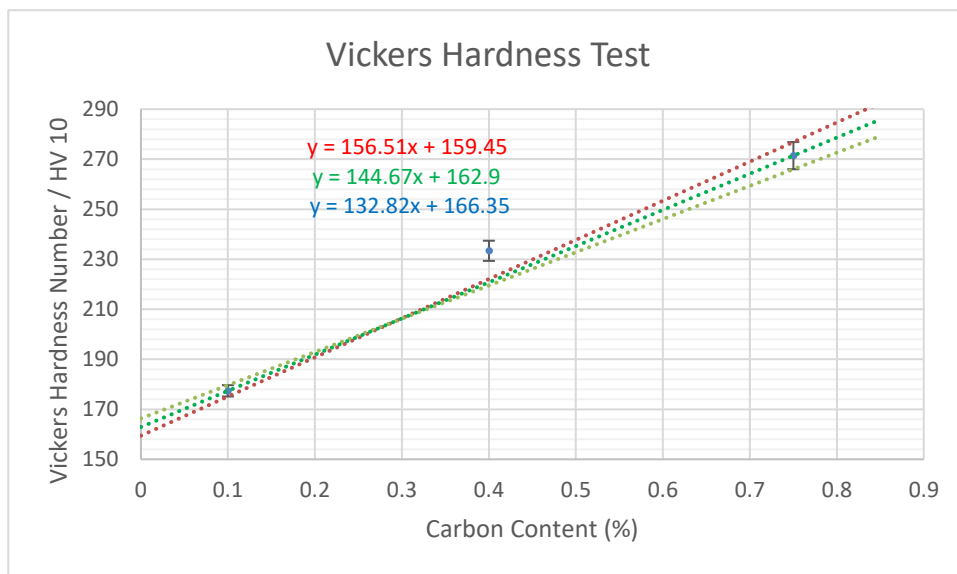


Figure 15 – HV10 - Carbon content Graph

Using the three line equations from figure 15, the hardness of ferrite and hardness of pearlite were estimated:

$$\text{Hardness value of ferrite} = 144.67 * (0.02) + 162.9 = 165.8 \pm 6$$

$$\text{Hardness value of pearlite} = 144.67 * (0.8) + 162.9 = 278.6 \pm 6$$

4) The three carbon contents being tested were 0.1%, 0.4%, 0.75%. Hence when slowly cooled from the γ state (shown by the red arrows in figure 16 below) to room temperature we can predict all three alloys to consist of Ferrite and Pearlite (different amounts of each).

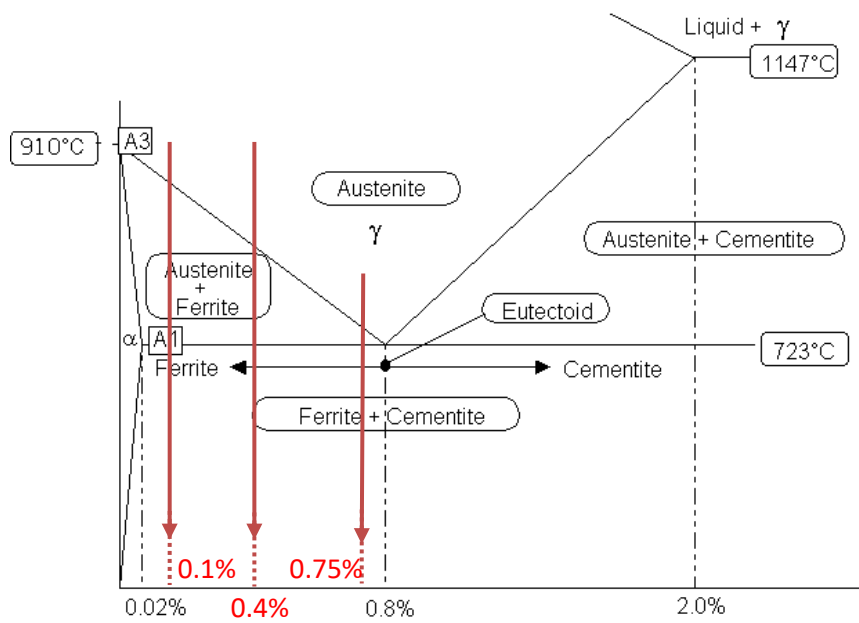


Figure 16 – Equilibrium phase diagram

Discussion

Experiment 1 - Tensile behaviour of aluminium and its alloys

Strengthening Mechanisms used in the experiment and their observed impacts:

- 1) Annealed pure aluminium – has the greatest ductility, with the largest plastic deformation region and a small elastic deformation region. In pure aluminium, dislocations can easily move through the microstructure and its slip planes. Pure aluminium also has the lowest UTS, other treatments increase the strength.
- 2) Cold working pure aluminium - Increases strength of the material and decreases ductility (the UTS of the cold worked aluminium was much greater than that of the annealed aluminium, and the percentage elongation was significantly lower). Theory explains that cold rolling extrudes aluminium between two rotating cylinders and flattens out its grain structure (figure 17). Work hardening aluminium by cold rolling causes its grains to slip, which makes aluminium more resistant to dislocation.

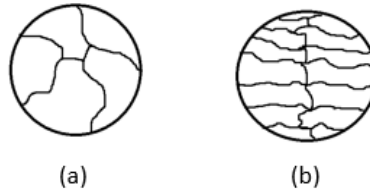


Figure 17 – Aluminium grain structure before (a) and after (b) the cold rolling process

- 3) Annealed aluminium-magnesium alloy – increased brittle behaviour than pure aluminium specimens, making it more difficult to plastically deform the material than pure aluminium samples. Increased strength – has a greater UTS than pure aluminium samples.
- 4) Two stage heat treatment of Duralumin (figure 18), low temperature precipitation hardening – led to a significant increase in UTS (almost four times the UTS value of the aluminium-magnesium alloy). This suggests that temperature in heat treatment has a major impact on mechanical properties of steel. During the precipitation hardening, copper diffuses into the aluminium. At a low temperature precipitation hardening, the copper grains are small, numerous and distributed evenly through the aluminium grains (figure 19).
- 5) Incorrect two stage heat treatment of Duralumin (figure 18), high temperature precipitation hardening – significant lower UTS value than obtained through mechanism 4. At a high temperature precipitation hardening, the copper grains are much larger, fewer and localised to grain boundaries (figure 19).

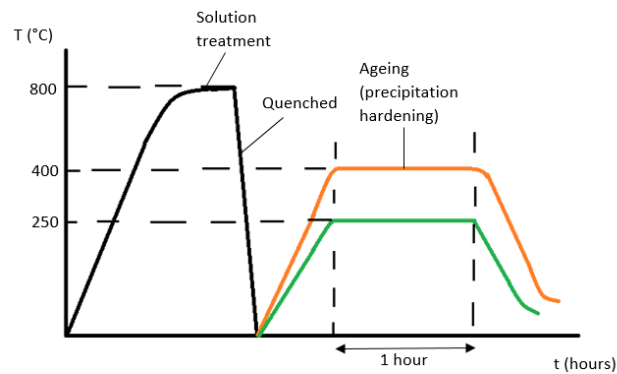


Figure 18 – Two stage heat treatment process. Temperature-time diagram.



Figure 19 – Copper (black) : Aluminium (white) distribution. Low vs High ageing temperature (left vs right)

Different processes can greatly impact the mechanical properties of aluminium and its alloys. From the table in Appendix B, it is seen that UTS is proportional to proof stress of aluminium. Hence, the strengthening impact is the same on tensile strengths and proof stresses. However, as seen above, there is a significant trade-off between strength and ductility. For aluminium to be ductile, the lattice must be able to dislocate and have a large plastic deformation. For aluminium to be stronger, it must be able to resist plastic deformation when high loads are applied. These properties imply that there is a trade off between ductility and strength. The results agree with this as the samples with higher UTS have lower ductility. For example, cold working increases strength at the cost of decreased ductility.

The only material suitable for welding would be the magnesium-aluminium alloy. This is because magnesium atoms enable lattice heat exchange. The other four aluminium materials cannot be used for welding. The heat-treated materials may be adversely affected by welding; high temperatures may cause undesirable effects to the microstructure of the aluminium. Whilst the pure aluminium specimens are too soft to be welded.

Pure aluminium and cold worked aluminium are appropriate materials for a range of applications, some examples include foils and corrosion resistant layers. The aluminium-magnesium alloy may be suited for use in manufacturing of drink cans because of its ductility and greater strength than pure aluminium. Heat treated aluminium is strong but has low density – it can be used in lightweight structures such as aircraft wings or orthopaedic technology (for hip-joint and knee cap replacements)

Experiment 2 - Investigating the hardness and microstructure of 'slowly cooled' carbon steel

The aim of this experiment was to investigate the hardness and microstructure of three samples of slowly cooled carbon steel. The Vickers Hardness test illustrates a strong, positive correlation between % carbon content and hardness number. This suggests that steels with greater carbon content have greater hardness. Since hardness correlates with strength, it can be suggested that strong steels have high % carbon content. However, the hardness value at 0.4% carbon content is very high and considered to be an anomaly. Therefore, the linear relationship between carbon content and hardness is questionable. Using a larger number of samples within the hypo-eutectoid range would improve the reliability of the trend observed. Using few samples reduces the credibility of the trend observed.

Microstructure analysis can explain the hardness trend observed from the Vickers hardness test. All three samples were cooled slowly from the austenite phase field to room temperature under equilibrium conditions (point 1 to point 3). At point 1, the steel sample is completely austenite. At point 2, primary ferrite forms at the grain boundaries of the austenite and the sample goes through a phase change. At point 3, microstructure contains regions of only ferrite and pearlite. Pearlite is a lamellar structure of cementite in secondary ferrite. However, lower carbon content steels would remain in the pure primary ferrite phase for a longer time period than higher carbon content steels. Therefore once steel reached the temperature of the pearlite region of the diagram, there was a lower composition of austenite left in the sample and thus less pearlite formed in lower carbon content samples. Pearlite is a lamellar structure of cementite in secondary ferrite. This microstructure creates more dislocations in the steel. At higher carbon contents, dislocations require more energy to move around (hence higher carbon steel better resists local plastic deformation) and thus, hardness is increased.

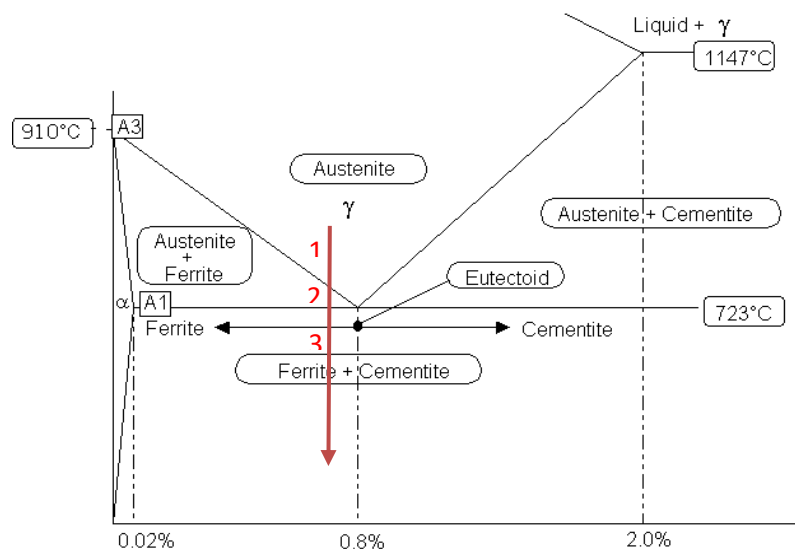


Figure 23 – Annotated Equilibrium phase diagram.

In real life, different percentages of carbon are used to achieve desirable mechanical properties of steel. In applications such as a welded footbridge, crankshaft and a chisel, it's important to consider the desirable properties before making a choice for the material:

1) Steel used for a welded footbridge must be suitable to carry people across the bridge, yet also must be resistant to corrosion and suitable for welding. Ideally, low carbon content steels are easily welded and cheap. High carbon content steels, whilst stronger, are expensive, brittle and less metallic (poor for welding). Low carbon content steels have high proportions of ferrite, which makes it easily welded but more likely to rust in wet conditions. Therefore, a compromise must be made between having low carbon content (ease of welding and low cost) and very low carbon content (likely to rust, have low strength). An intermediate carbon content would be optimal – perhaps 0.3 % carbon steel.

2) Steel used for a crankshaft must have high fatigue resistance (to withstand repeated loading) and be able to withstand high temperatures. Low carbon contents around 0.1% would be too soft to withstand high stresses and therefore would not be recommended. Whereas very high carbon steels around 0.7% aren't suitable either. At high temperatures, high carbon steels form a very hard, brittle form of steel crystalline structure called martensite. Being brittle is not desirable. Therefore, a carbon content of around 0.6% would provide suitable properties to resist fatigue failure and greater hardness can be achieved by methods such as layering, case hardening or heat treatment.

3) In a chisel, the tip must be hard so that it can swiftly cut through materials whilst the bottom must be tough to withstand regular repeated impact. Since the mechanical properties required are slightly different, there are many ways to approach the application. One way would be to use different steel alloys for the two parts – high carbon content steel for the tip and intermediate carbon content steel for the bottom. However, a more reasonable approach would be to process the steels in different conditions ie. Using heat treatment or quenching the tip to increase strength and cold working to increase the toughness of the bottom. Recommended carbon content would be around 0.65-0.7 % carbon content, where the tip undergoes heat treatment and the bottom is cold worked.

Conclusion

The purpose of the investigation was to investigate the behaviour and structure of different types of aluminium and steel. The investigation successfully illustrated several factors that affect the mechanical properties and structure of steel and aluminium.

The experiment involving the tensile test of five different aluminium specimens displayed the impact of strengthening mechanisms on the strength, ductility and mechanical properties of aluminium. The green specimen went through a two-stage heat process and therefore had the highest value of UTS. The order of strength follows as: green, black, red, pink, and blue, where the pure aluminium samples were the weakest. Other than types of treatments, it was also discovered that temperature has a significant impact on the strength of the material as the incorrectly heat treated aluminium sample was much weaker than the first heat treated aluminium sample. For the aluminium-magnesium alloy, strength was increased for a small decrease in ductility. The magnesium atoms make it more difficult for dislocations to move through the aluminium sample and therefore increase the total energy input required to propagate cracks in the material. The UTS of aluminium and its ductility seem to be inversely correlated – brittle materials tended to have higher strength. Further proof is provided by the failure sound and the percentage elongation of the five samples. However, this evidence is inconclusive and further testing needs to be done. One improvement to the experiment could be to take a wider range of specimens with different treatments to further investigate the trends.

The second experiment demonstrated a positive correlation between the carbon content of a steel and its hardness. Increased levels of pearlite in higher carbon content samples create dislocations which make the material more resistant. However, the reliability of this trend is questionable since only three data values were collected. An improvement may be to test more than three samples at a greater range of carbon contents. In terms of real life application, recommendations made include using 0.3% carbon steel for the welded footbridge (compromise between hardness and ductility), using 0.6% carbon steel with recommended heat treatments for the crankshaft (to increase strength) and using 0.7% carbon steel with recommended heat treatments (to increase strength) and cold working (to increase toughness) for the two parts of the chisel (the tip and the bottom).

Appendices

Section A

$$1) \quad \text{Stress} = \frac{\text{Force}}{\text{Cross-sectional Area}}$$

The force on the specimen is found as the load measurement from the tensile test of the specimen (given uncertainty of $\pm 0.5\%$).

Cross-sectional area is calculated by multiplying the thickness ($\pm 0.005 \text{ mm}$) and width ($\pm 0.005 \text{ mm}$) of the specimen.

Therefore, uncertainty analysis shows:

$$\text{Area} = 7.47 * 0.94 = 7.02 \text{ mm}^2$$

$$\frac{0.005}{7.47} + \frac{0.005}{0.94} = \frac{\Delta A}{7.02} \text{ so } \Delta A = 0.04 \text{ (1sf)}$$

$$\text{Area} = 7.02 \pm 0.04 \text{ mm}^2$$

Taking an arbitrary load value:

$$\text{Stress} = \frac{16.73682}{7.02} = 2.38 \text{ MPa}$$

Error propagation:

$$\frac{\Delta \sigma}{2.38} = 0.01 + \frac{0.04}{7.02} \text{ so } \Delta \sigma = 0.025 = 0.03 \text{ (1sf)}$$

2) Lever rule:

$$X_{\alpha p} = \frac{C_{\text{pearlite}} - \% \text{carbon content in sample}}{C_{\text{pearlite}} - C_{\alpha}} \text{ and } X_{\text{pearlite}} = \frac{\% \text{carbon content in sample} - C_{\alpha}}{C_{\text{pearlite}} - C_{\alpha}}$$

For example, for 0.1 % carbon content, the fraction of ferrite present is given by:

$$X_{\alpha p} = \frac{0.8 - 0.1}{0.8 - 0.02} = 0.897 = 89.7 \%$$

Section B

| |
|---|
| Table 5 – Tensile test of processed Aluminium samples |
|---|

| Specimen | % elongation | UTS (MPa) | 1% Proof Stress | Fracture Noise | Fracture Angle (°) | Necking |
|----------|--------------|-----------|-----------------|----------------|--------------------|---------|
| Blue | 33.3 | 43 ± 1 | 35 ± 1 | Silent | 45 | Yes |
| Pink | 7.7 | 113 ± 2 | 110 ± 2 | Quiet sound | 45 | Yes |
| Red | 23.3 | 170 ± 3 | 100 ± 2 | Small Click | 45 | Yes |
| Green | 6.7 | 445 ± 7 | 412 ± 6 | Loud Click | 90 | No |
| Black | 16.7 | 195 ± 3 | 150 ± 2 | Click | 90 | No |

References

- 1) Blackman, B. R. (2016). *The Properties of Engineering Alloys*. London: Imperial College London
- 2) Figures 2 & 3: "Standard Tensile Testing Machine"
<https://www.labtestmachines.com>
- 3) Figure 4: "Parts of a micrometer"
http://www.kanabco.com/vms/measure_mic_basic/measure_mic_basic_02.html
- 4) Figure 6: "Flat Aluminium Tensile Specimen"
https://upload.wikimedia.org/wikipedia/commons/7/71/Tensile_specimen-round_and_flat.jpg
- 5) Figure 8: "Bakelite Mount"
<http://cdnstruersproduction.azureedge.net/-/media/Struers-media-library/Products/Mounting/Mounting-consumables/Hot-Mounting-Bakelite-356x234-px.jpg?h=234&la=en&w=356&hash=4A305E2772FC733D79F51C98DAB0DB3804703B34>
- 6) Figure 9: "Nital Solution for Etching"
<http://www.etchantstore.com/images/Nital%20Etch%20Kit%20rev%201.jpg>
- 7) Figure 10: "Polisher"
http://www.digitalhardnesstesters.com/photo/pl11632175-double_disc_metallurgical_specimen_grinder_polisher_with_diameter_200mm.jpg
- 8) Figure 11: "Vickers Hardness setup"
<http://user.china-dirs.cn/k062/user026/uploadfile/20161210121021677.jpg>
- 9) Figure 12: "Phase diagram"
<http://www.gowelding.com/met/carbon1.gif>